

Establishment and correction of an Echelle cross-prism spectrogram reduction model

Rui Zhang^{a,b,*}, Bayanheshig^a, Xiaotian Li^{a,*}, Jicheng Cui^a

^a Grating Technology Laboratory, Changchun Institute of Optics and Fine Mechanics and Physics, Chinese Academy of Sciences, Changchun, Jilin 130033, China

^b University of Chinese Academy of Sciences, Beijing 100049, China

ARTICLE INFO

Keywords:

Echelle cross-prism spectrometer
Spectrogram reduction model
Two-dimensional spectrum

ABSTRACT

The accuracy of an echelle cross-prism spectrometer depends on the matching degree between the spectrum reduction model and the actual state of the spectrometer. However, the error of adjustment can change the actual state of the spectrometer and result in a reduction model that does not match. This produces an inaccurate wavelength calibration. Therefore, the calibration of a spectrogram reduction model is important for the analysis of any echelle cross-prism spectrometer. In this study, the spectrogram reduction model of an echelle cross-prism spectrometer was established. The image position laws of a spectrometer that varies with the system parameters were simulated to the influence of the changes in prism refractive index, focal length and so on, on the calculation results. The model was divided into different wavebands. The iterative method, least squares principle and element lamps with known characteristic wavelength were used to calibrate the spectral model in different wavebands to obtain the actual values of the system parameters. After correction, the deviation of actual x- and y-coordinates and the coordinates calculated by the model are less than one pixel. The model corrected by this method thus reflects the system parameters in the current spectrometer state and can assist in accurate wavelength extraction. The instrument installation and adjustment would be guided in model-repeated correction, reducing difficulty of equipment, respectively.

© 2017 Elsevier B.V. All rights reserved.

1. Introduction

Recently, spectrometers have been widely used in many fields, including agriculture, medicine, and astronomy [1–6]. Among them, the echelle cross-prism spectrometer has the advantages of small volumes and high resolution and has thus become a research hotspot [4,7–10]. The main dispersion element (echelle grating) of the echelle cross-prism spectrometer has a high diffraction order and large blazing angle [11], which produces a high dispersion rate and resolution. However, the high diffraction order leads to overlapping diffraction that makes the spectrometer unusable. To solve this problem, a cross-dispersion element is added after the echelle grating [12,13] to acquire two-dimensional spectrum without overlapping spectral lines. In this two-dimensional spectrogram, the intensity of the target light spot and its image plane position is known. The two-dimensional spectrum has to be transformed into a one-dimensional spectrum. This means that the relationship between the light spot intensity and its image plane position has to be turned into the relationship between the light spot intensity and its wavelength.

In general, a spectrogram reduction model is used to transform a two-dimensional spectrum into a one-dimensional spectrum [14–16]. This model constructs the relationship between the image coordinates and the wavelength values. The relationship between coordinates and the characteristic spot intensity can be acquired by the echelle cross-prism spectrometer. So the relationship between the characteristic spot intensity and wavelength can be deduced, the wavelength can be calculated.

However, this model does not always accurately compute the position of the image plane. This is because the changes in the actual state of the spectrometer will result in changes in the actual parameter values (prism incidence angle, grating incidence angle, grating offset angle, focal length, etc.). If the model with the fixed system parameter values is used to calculate the entire optical system, the spectrogram reduction model may not match the actual state of the spectrometer. This means that the results calculated by the spectral reduction model will be inaccurate, as will the wavelength calculation. Keling [17] has studied the effects of temperature and humidity changes on wavelength calculation

* Correspondence to: No.3888 Dong Nanhu Road, Changchun, Jilin 130033, China.
E-mail addresses: zhangrui_grating@163.com (R. Zhang), lixt_1981@163.com (X. Li).

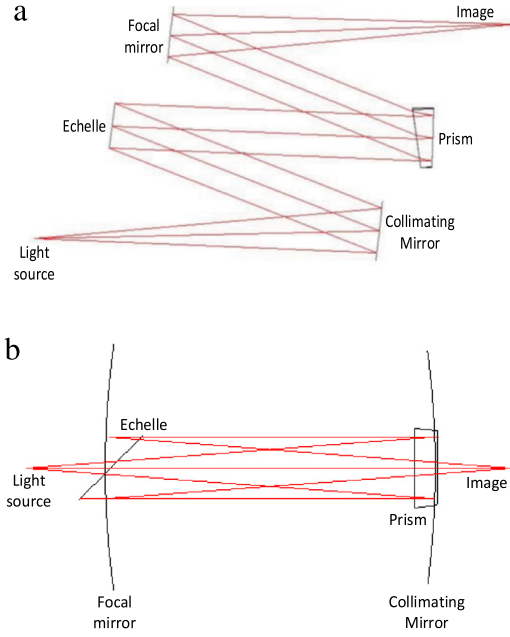


Fig. 1. Structure of the echelle cross-prism spectrometer used in this study (a) XZ plane (b) YZ plane.

accuracy. It can change the optical element status in the spectrometer through transportation, vibration and error of adjustment. This will then change the imaging position and the previously established spectral reduction model will not match the actual situation of the spectrometer and result in an inaccurate wavelength calculation.

Therefore, this paper established spectrogram reduction model. Then, the effect of model parameters on the accuracy of model calculation is simulated when the input parameters in the model are in error with the actual parameters of the spectrometer. The simulation results show that the deviation between the input parameters and the actual parameters will have a great influence on the final model calculation results. Therefore, this paper corrects the model. The iterative method is used to change the value of input parameters in a certain range, and then obtain a number of spectral reduction model. The image plane coordinates of these models are compared with the actual coordinates according to the least square principle (Minimize the sum of squared errors of the computations). Finally, the model with the least residual error is the corrected model, whose input parameters are the parameters after correction.

2. Establishment and correction of the spectrogram reduction model

2.1. The establishment of the spectrogram reduction model

The spectrometer has a C-T type structure (Fig. 1).

The dispersion direction of the prism is perpendicular to the dispersion direction of the echelle. Assume that the prism dispersion is in the horizontal (x) direction and the echelle is in the vertical (y) direction. Establishment a spectral reduction model. Firstly, study on the echelle dispersion direction. The echelle grating is placed in the echelle cross-prism spectrometer with a certain offset angle. The diffraction equation can be expressed as:

$$d(\sin \alpha + \sin \beta) \cos \omega = m\lambda \quad (1)$$

where d is the groove spacing, α is the incidence angle of the echelle grating, β is the diffraction angle of the echelle grating, ω is the grating offset angle, m is the grating diffraction order, and λ is the incident light wavelength.

The light at the blazing angle emitted from the grating is transmitted to the center of the image plane. The angle at the grating between the arbitrary lights and the light on the center of the image plane can be expressed by:

$$\Delta\beta = \beta - \beta_0 \quad (2)$$

where β_0 is the diffraction angle of the light on the center of the image plane, and $\Delta\beta$ is the angle between arbitrary lights and the light incident on the center of the image plane.

The distance between the position of the arbitrary lights on the image plane and the center of the image plane in the y direction can be expressed as:

$$y = \frac{\Delta\beta}{f \cos \omega} \quad (3)$$

where y is the distance between the position of arbitrary lights on the image plane and the center of the image plane in the y direction, and f is the system focal length. Based on Eqs. (1)–(3), the relationship between the wavelength and y -coordinates can be established and the relationship expressed as:

$$\lambda = \frac{d}{m} \left[\sin \alpha + \sin \left(\beta_0 + \frac{y}{f \cos \omega} \right) \right] \cos \omega. \quad (4)$$

For the prism dispersion direction, the prism exit angle corresponding to the light at the center of the image plane can be deduced by the geometric optics theory. The prism exit angle of the arbitrary lights can be calculated using the law of refraction. Thus, the angle on the prism between the arbitrary lights and the light on the center of the image plane can be determined. The distance between the position of arbitrary lights on the image plane and the center of the image plane in the x direction can be expressed as:

$$x = f * (\theta - \theta_0) \quad (5)$$

where x is the distance between the position of the arbitrary lights on the image plane and the center of the image plane in the x direction, θ is the exit angle of arbitrary lights on the prism, and θ_0 is the prism exit angle corresponding to the light at the center of the image plane. The prism is made of materials that can be transmitted through ultraviolet light (JGS1). Based on the law of refraction, the prism exit angle is related to the prism refractive index with different wavelengths corresponding to different refractive indices [15]:

$$n^2 = 2.1049 + \frac{0.0087}{\lambda^2 - 0.0111} - 0.0103\lambda^2 \quad (6)$$

where n is the refractive index, λ is the wavelength value and the adaptive band range of Eq. (6) is 190–600 nm.

Using Eq. (6), the relationship between a wavelength and its x -coordinates can be established, and then expressed as:

$$x = f * \tan \left\{ \arcsin \left\{ n(\lambda_1) \sin [2\delta - \sin^{-1} i / n(\lambda_1)] \right\} - \arcsin \left\{ n(\lambda_0) \sin [2\delta - \sin^{-1} i / n(\lambda_0)] \right\} \right\} \quad (7)$$

where λ_1 and λ_0 are the wavelengths with output angles θ and θ_0 , respectively, i is the incidence angle of the prism, δ is the apex angle of the prism, and $n(\lambda)$ is the wavelength-dependent refractive index.

Finally, according to the Eqs. (4) and (7), the relationship between the wavelengths and the x - and y -coordinates of the image plane can be confirmed. Put the results into a matrix, the number of rows and columns of the matrix correspond to the X and Y coordinate values, and the value of the matrix corresponding to the wavelength.

$$\lambda_{X,Y} = \begin{bmatrix} \lambda_{X_1 Y_1} & \lambda_{X_1 Y_2} & \cdots & \lambda_{X_1 Y_q} \\ \lambda_{X_2 Y_1} & \lambda_{X_2 Y_2} & \cdots & \lambda_{X_2 Y_q} \\ \vdots & \vdots & \ddots & \vdots \\ \lambda_{X_p Y_1} & \lambda_{X_p Y_2} & \cdots & \lambda_{X_p Y_q} \end{bmatrix} \quad (8)$$

where p and q are the number of pixels in the Charge-coupled Device (CCD) detector.

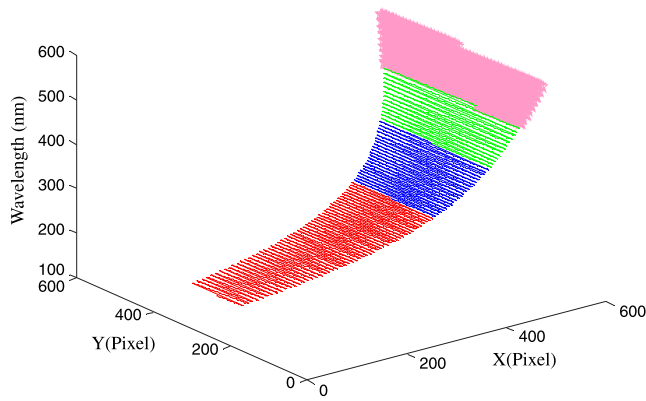


Fig. 2. Spectral reduction model schematic.



Fig. 3. The actual spectrum of mercury lamp acquired by echelle cross-prism spectrometer.

In this study, the echelle cross-prism spectrometer was used which the wavelength range was 250–600 nm and resolution was 0.02 nm. The established spectral reduction model is divided into different wavebands with the wavelength interval of the model less than the instrument resolution. The model wavelength interval was set to 0.01 nm and the wavelength range to four segments (250–300, 300.01–400, 400.01–500 and 500.01–600 nm) (Fig. 2). The y - and x -coordinates indicate the position of the light in the image plane, and the z -coordinates indicates the wavelength value of the light. The range of y - and x -coordinates ranges from 0 to 512. The spectrometer parameters used in the model are shown in Table 2. (The design parameters of spectrometer.)

The Fig. 3 is the two dimensional spectrum of mercury (Hg) lamp acquired by the CCD-array detector. The gray value of the spot is its light intensity value, and the position of the spot can be expressed by X and Y coordinates.

By combining the spectrum reduction model with the actual two-dimensional spectrum, a one-dimensional spectrum of the incident light wavelength with respect to its light intensity was obtained.

2.2. The correction of the spectrogram reduction model

Any spectrometer can have installation errors, so the condition of the internal optical element may not match the actual design value. When using an echelle cross-prism spectrometer, occurrences in the external environment, such as vibrations during transport, could lead to changes in the state of its internal optical elements. These will lead to high precision imaging position changes and the calculation results of the model with the ideal design parameters are not consistent. The wavelength calculation would be inaccurate. Therefore, during the use of an echelle cross-prism spectrometer, the spectrogram reduction model should be calibrated periodically.

Table 1

Echelle cross-prism spectrometer parameters.

Parameters of the echelle cross-prism spectrometer	
Numerical aperture	0.0712
Prism incidence angle	10.44°
Grating groove density	54.5 g/mm
Grating incidence angle	46.6°
Grating offset angle	8°
Focal length	262 mm

Firstly, through the relationship between the initial model size and the detector size, the variation range of the four parameters (grating incidence angle, prism incidence angle, grating offset angle, system focal length) can be obtained. Beyond this range, the resulting model will exceed the receiver's range of acceptance and needs the mechanical adjustment. By iterative method, the input parameters (grating incidence angle, prism incidence angle, grating offset angle, system focal length) are changed sequentially, and several models of spectral reduction are calculated. The image plane coordinates of these models are compared with the actual coordinates according to the least square principle (Minimize the sum of squared errors of the computations). Finally, the model with the least residual error is the corrected model, whose input parameters are the parameters after correction.

The steps for the segment correction of the spectrogram reduction model are: (1) Select the element lamp with known wavelength; (2) Measure the selected element light with the echelle cross-prism spectrometer and extract the actual position coordinate information (x_h , y_h) of each characteristic spot using the algorithm; (3) The characteristic wavelength corresponding to the image coordinates calculated by the model depends on the input parameters of the model, such as the grating incidence angle, prism incidence angle, and system focal length. By changing the input parameters, the model computes a series of position coordinates (x_{hk} , y_{hk}), which is then compared to the actual image coordinates (x_h , y_h):

$$H_k = \sum_{i=1}^h (x_{hk} - x_h)^2 + \sum_{i=1}^h (y_{hk} - y_h)^2, \quad h = 1, 2 \dots h, k = 1, 2 \dots k \quad (9)$$

where h represents the different known spots, x_h , y_h represents the different known spot coordinates, k represents the different input parameters, and x_{hk} , y_{hk} are the different known spot coordinates calculated by the different input parameters of the model.

The least squares principle completely compensates for error, which effectively reduces the impact of random errors, and thus produces the most reliable results. The sum of squared residuals is minimized according the principle of least squares. The input parameter that calculates the minimum value (H_k) is selected, and this group of parameters is used as the final input parameters of the model, which completes the model calibration.

3. Simulation analysis

The parameters of the echelle cross-prism spectrometer are shown in Table 1.

The influence of the system parameter changes on the imaging position of the spectrometer was simulated and analyzed (Fig. 4). Among them, the x - and y -coordinates are the image plane coordinates corresponding to the known wavelength, and the z -coordinates are the known wavelength corresponding to the x and y -coordinates deviation (Fig. 4a and b). When the refractive index of prism is changed. The y -coordinates of the image plane are transformed by the translation, the absolute of x -deviation increases linearly with the increase in the refractive index of prism (Fig. 4c). Usually, the model calculation error is controlled within one pixel to meet the requirement of accuracy. When the deviation is 0.00022, the x -coordinates change by a pixel. In contrast, changes in the prism refractive index has slightly effect on y -values, which does not affect the final result (Fig. 4c).

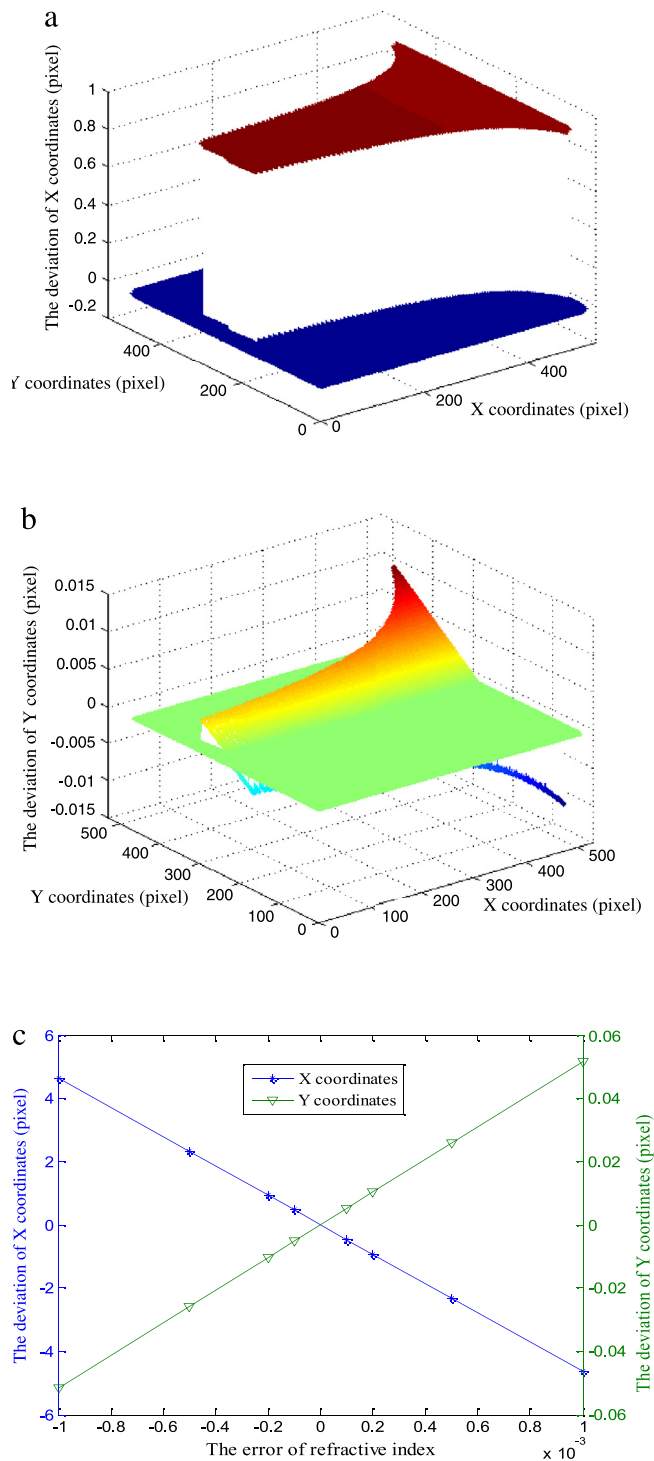


Fig. 4. Effect of the refractive index of prism on the image plane coordinate. (a) The deviation of x -coordinates when the prism refractive index changes 0.0002. (b) The deviation of y -coordinates when the prism refractive index changes 0.0002. (c) The effect of prism refractive index changes.

Similarly, when incident angle of the grating is changed. The x -coordinates are unchanged, but the y -coordinates are transformed by the translation, and the shape is similar to Fig. 4a. Moreover, the absolute of y -deviation increases linearly with the increase of the grating incident angle and the shape is just like Fig. 4c (Y coordinates). When the deviation is $11.35''$, the y -coordinates change by a pixel.

Furthermore, when the prism incidence angle and the grating offset angle are changed, the x -coordinates are transformed by the translation, and the shape is similar to Fig. 4a. The absolute of x -deviation increases linearly with the increase in the system parameters (prism incidence angle and the grating offset angle) and the shape is similar Fig. 4c (Y coordinates). When the deviation is $9.97''$ and $10.31''$, the x -coordinates change by a pixel. The changes in the prism incidence angle and the grating offset angle have no effect on the y -values.

The influence of the system focal length on the image plane coordinates is different from other system parameters (Fig. 5). When the focal length is changed, the coordinates of the two sides of the image plane change in two directions (positive and negative). In general, the closer to the edge of the image plane, the greater the coordinate change. When the focal length deviation reaches 0.78 mm, the y -coordinate of the image plane changes by a maximum of a pixel and when it is 4.09 mm, the x -coordinate changes by a pixel.

As shown by Figs. 4 and 5, system parameter variations have a large influence on the imaging position.

When the refractive index of the prism and the focal length of the system have a certain deviation, the deviation of the model results in different positions of the image surface is different, so they cannot compensate each other. The deviation of grating incidence angle, prism incident angle and grating offset angle will cause the translation error of the model. The grating incidence angle influences the calculation of the Y coordinate. The prism incidence angle and the grating offset angle affect the calculation of the X coordinate. Therefore, the deviation of the prism incident angle can compensate the deviation produced by the grating offset angle. For example, when the deviation of the prism incident angle causes the model to calculate the deviation of -1 pixel, the deviation of the grating offset angle causes the model to calculate the deviation of the $+1$ pixel in the X direction. This can compensate the calculated deviations from each other. The X coordinate calculated by the final model is accurate.

When the deviation between model calculation coordinates and the actual coordinates is one pixel, the corresponding wavelength extraction error as shown in Fig. 6. The dispersion ability of grating in short waveband is stronger. Therefore, when the coordinate calculation error is a pixel, the long waveband extraction error is larger than the short waveband. The prism eliminates the spectral order overlapping in X direction and the dispersion ability in short waveband is stronger than long waveband. So, the wavelength becomes shorter when the distance in pixels between two adjacent wavelengths along the x -axis becomes longer in the short wave direction. The longest distance is six pixels, and the shortest is two pixels. Thus, as stated above, when the error in the X position is more than one pixel, the wavelength calibration model will inaccurate.

Therefore, it is necessary to correct the spectral reduction model periodically.

4. Experimental results

To calibrate the model and compare it to the actual spectrometer state, we acquired spectrograms for additional element lamps, including zinc (Zn), aluminum (Al), magnesium (Mg), chrome (Cr), and calcium (Ca). In the spectrum, the gray value of the light spot corresponds to its light intensity, and the location of the spot in the spectrum corresponds to its image plane coordinates (x, y). The centroid extraction algorithm is used to extract the coordinates of the image plane corresponding to the known wavelength spot in the spectrum. According to iterative method and least square principle, the sum of the squares of errors between the model calculated coordinates and the extracted coordinates is minimized by modifying the model input parameters (grating incidence angle, prism incidence angle, grating bias angle, system focal length). Therefore, we can confirm the model input parameters of model and the actual status of the spectrometer. The deviation between the actual coordinates and model calculated coordinates in the X and Y direction

Table 2
The parameters deviation of echelle cross-prism spectrometer.

	Grating incidence angle (°)	Prism incidence angle (°)	Grating offset angle (°)	Focal length (mm)
The design parameters of spectrometer	46.6	10.44	8	262
The actual parameters of spectrometer	46.607	10.442	7.999	262.8

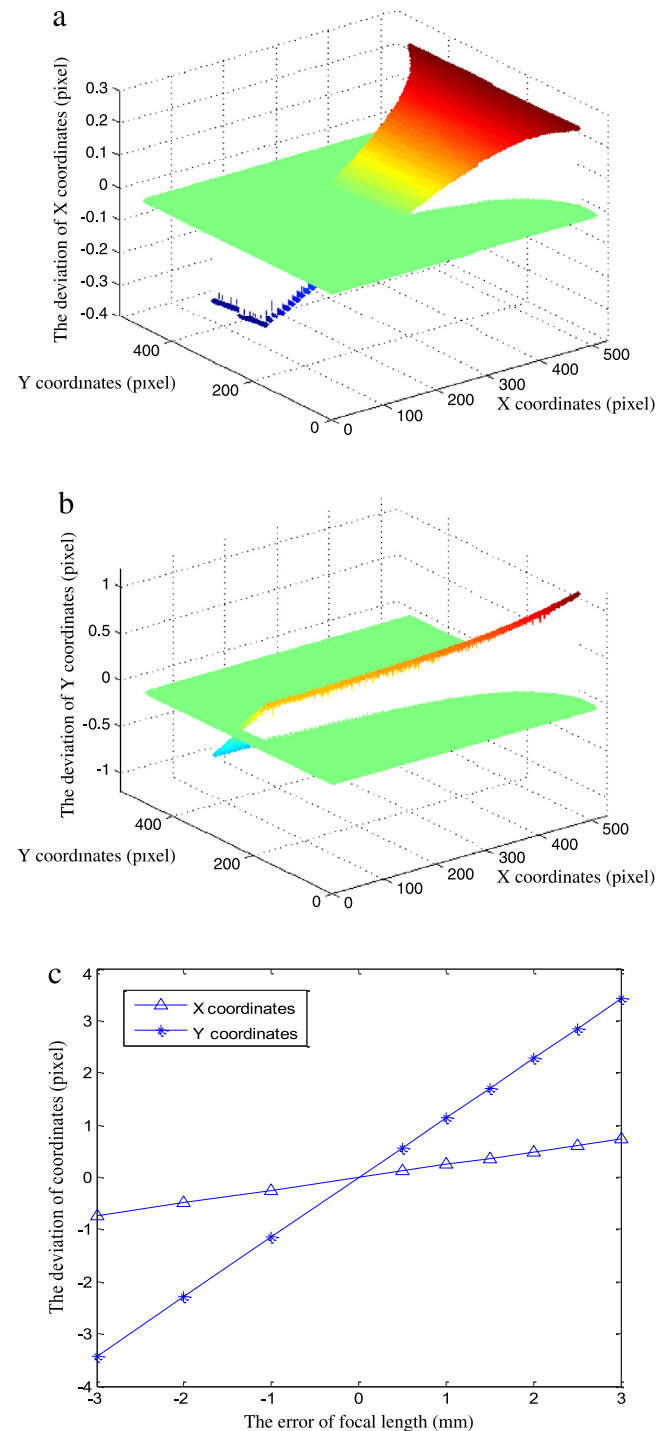


Fig. 5. Effect of the focal length on the image plane coordinates. (a) The deviation of *x*-coordinates when the focal length change 1 mm. (b) The deviation of *y*-coordinates when the focal length change 1 mm. (c) The effect of focal length changes.

is less than one pixel (Fig. 7), which indicates that the model reflects the actual state of the spectrometer. Therefore, the spectra can be accurately calculated with the reduction model.

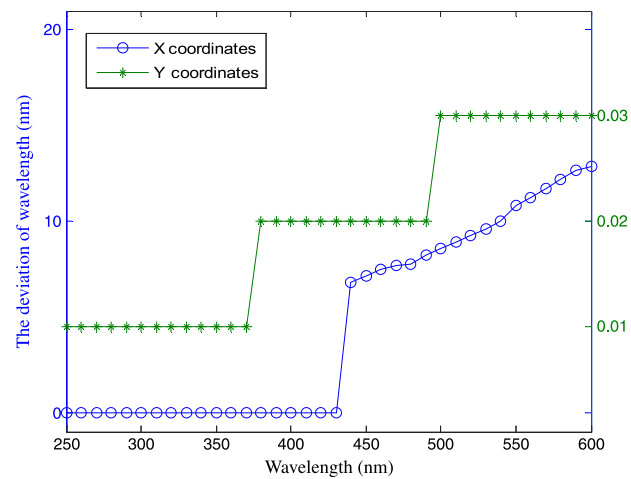


Fig. 6. The effect of coordinates deviation on the calibration accuracy.

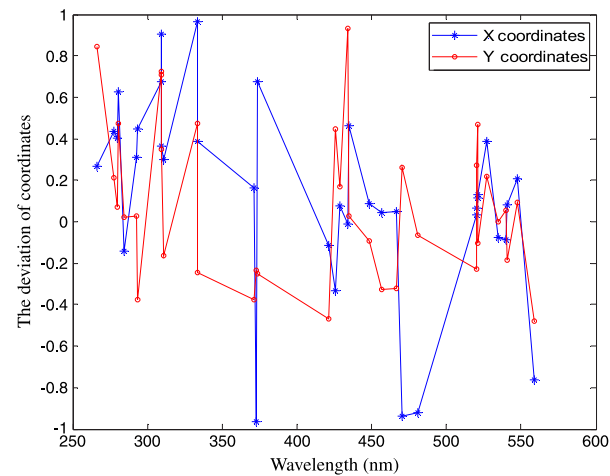


Fig. 7. The deviation between actual coordinates and model calculated coordinates.

The instrument parameters as shown in Table 2.

Finally, the accuracy of the corrected spectral reduction model was verified by using a mercury lamp with a clean characteristic spot (Fig. 3). Before correction the model, the deviation between calculated coordinates and the actual coordinates of the characteristic spot from the mercury lamp is shown in Fig. 8. The maximum deviation is three pixels. After correction the model, the deviation between calculated coordinates and the actual coordinates of the characteristic spot from the mercury lamp is shown in Fig. 9. In both *x* and *y* directions, the position deviation is less than one pixel, which demonstrates the model accurately reflects the actual state of the spectrometer. This is an important finding to guide instrument debugging.

Finally, the one-dimensional spectrum can be obtained by the two-dimensional spectrum and reduction model, (Fig. 10). At the characteristic wavelength of 577.067 nm, the wavelength calibration error is 0.087 nm before correction the model and the wavelength calibration error is 0.003 nm after correction the model (Fig. 11).

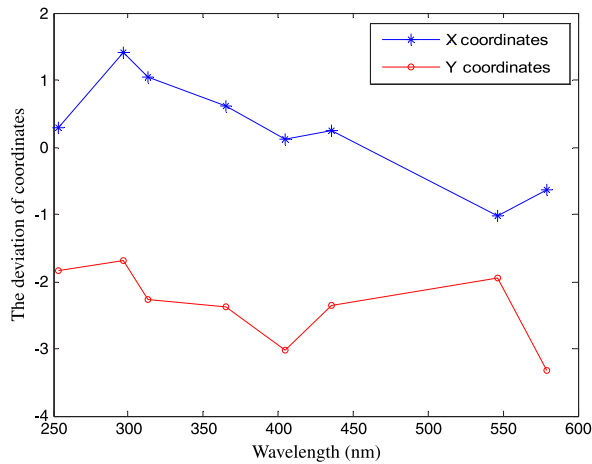


Fig. 8. The deviation between actual coordinates and model calculated coordinates from the mercury lamp before correction.

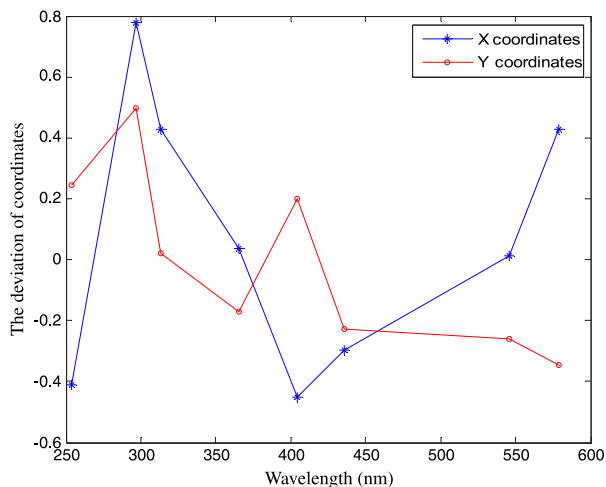


Fig. 9. The deviation between actual coordinates and model calculated coordinates from the mercury lamp after correction.

5. Conclusions

There are many factors that can lead to the state of the spectrometer different from the design values, including the error of spectrometer adjustment. These can seriously affect the wavelength calibration accuracy of an echelle cross-prism spectrometer. This paper establishes a spectral reduction model for an echelle grating spectrometer that can invert the instrument system parameters. The simulation results show that the system parameter changes strongly influence the imaging position of the spectrometer. In order to improve the accuracy of the model calculation results, the automatic calibration method was studied. As a first step, known wavelength from an element lamp that corresponded to a characteristic spot position was determined. Using known wavelengths and their position, the model input parameters were determined and the actual status of the spectrometer was known. Finally, the model was compared with the actual state of the spectrometer to confirm the calibration of the spectrum reduction model was completed. After the calibration, the coordinate deviation calculated for the x and y directions was less than one pixel. This method improves the accuracy of the spectrum reduction model and confirms the state of the spectrometer while calibrating the model. This improves the effectiveness of spectrometer installation and adjustment, reduces the difficulty of spectrometer installation and improves the calibration accuracy of the spectrometer.

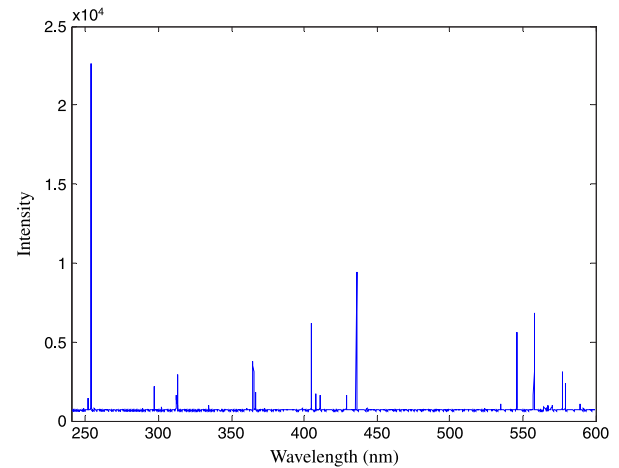


Fig. 10. The one-dimensional spectrum of mercury lamp.

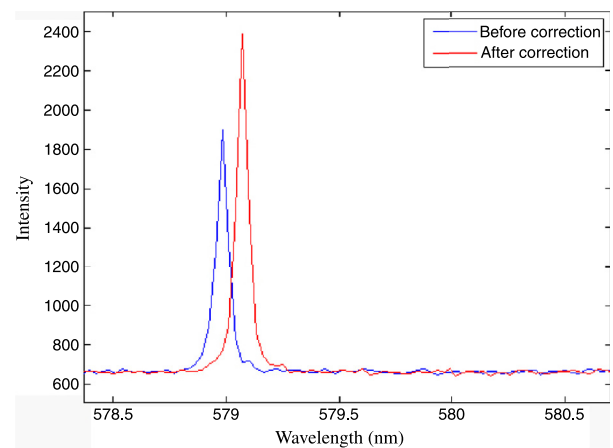


Fig. 11. The wavelength extraction error of mercury lamp.

Acknowledgments

The authors acknowledge supports from the Chinese Finance Ministry for the National R&D Projects for Key Scientific Instruments (grant ZDYZ2008-1), from National Natural Science Foundation of China (grant 61505204), from Ministry of national science and technology for National Key Basic Research Program of China (grant 2014CB049500), and from National key scientific Instrument and Equipment development projects in china (2014YQ120351).

References

- [1] P. Wang, R. Menon, Computational spectrometer based on a broadband diffractive optic, *Opt. Express* 22 (2014) 14,575–14,587.
- [2] B. Redding, S.F. Liew, R. Sarma, H. Cao, Compact spectrometer based on a disordered photonic chip, *Nat. Photonics* 7 (2013) 746–751.
- [3] B. Redding, H. Cao, Using a multimode fiber as a high-resolution, low-loss spectrometer, *Opt. Lett.* 37 (2012) 3384–3386.
- [4] C. Vannahme, M. Dufva, A. Kristensen, High frame rate multiresonance imaging refractometry with distributed feedback dye lasersensor, *Light Sci. Appl.* 4 (2015) e269.
- [5] B. Redding, S.F. Liew, R. Sarma, H. Cao, Compact spectrometer based on a disordered photonic chip, *Nat. Photonics* (2013) doi:10.1038.
- [6] B. Redding, S.M. Popoff, H. Cao, All-fiber spectrometer based on speckle pattern reconstruction, *Opt. Express* 21 (2013) 6584–6600.
- [7] L. Xu, M.A. Davonport, M.A. Turner, T. Sun, K.F. Kelly, Compressive Echelle spectroscopy, *Proc. SPIE* 8165 (2011) 81650E.

- [8] F. Pascal, D. Menut, R. Brennetot, Analysis by laser-induced breakdown spectroscopy of complex solids, liquids, and powders with an echelle spectrometer, *Appl. Opt.* 42 (30) (2003) 6029–6035.
- [9] S.V. Bykov, High-throughput. high-resolution echelle deep-UV raman spectrometer, *Appl. Spectrosc.* 67 (8) (2013) 873–883.
- [10] P. Xie, Z. Ni, Y. Huang, D. Zhang, Y. Zhang, Application research progress in the echelle grating, *Laser J.* 30 (2009) 4–6.
- [11] Li Xiaotian, Yu Haili, 300 mm ruling engine producing gratings and echelles under interferometric control in China, *Appl. Opt.* 54 (7) (2015) 1819–1826.
- [12] O. Furxhi, L.M. Daniel, J.B. David, Echelle crossed grating millimeter wave beam scanner, *Opt. Express* 22 (13) (2014) 16393–16407.
- [13] O. Korablev, F. Montmessin, Compact echelle spectrometer for occultation sounding of the Martian atmosphere: design and performance, *Appl. Opt.* 52 (5) (2013) 1054–1065.
- [14] Y. Tang, S. Chen, Bayanheshig, J. Cui, J. Chen, Spectral reducing of cross-dispersed echelle spectrograph and its wavelength calibration, *Opt. Precis. Eng.* 18 (2010) 2130–2136.
- [15] R. Zhang, Bayanheshig, Wavelength calibration model for prism-type echelle spectrometer by reversely solving prism's refractive index in real time, *Appl. Opt.* 55 (15) (2016) 4153–4158.
- [16] L. Yin, Bayanheshig, High-accuracy spectral reduction algorithm for the échelle spectrometer, *Appl. Opt.* 55 (13) (2016) 3574–3581.
- [17] L. Keling, Gary M. Hieftje, Investigation of wavelength calibration for an echelle cross-dispersion spectrometer, *J. Anal. At. Spectrom* 18 (2003) 1177–1184.